An Adaptive Soft Sensor for On-Line Monitoring the Mass Conversion in the Emulsion Copolymerization of the Continuous SBR Process

*Carlos I. Sanseverinatti, Mariano M. Perdomo, Luis A. Clementi, Jorge R. Vega**

C. I. Sanseverinatti, M. M. Perdomo, J. R. Vega

Institute of Technological Development for the Chemical Industry (INTEC, UNL-CONICET), Ruta Nacional 168, Km. 0, Paraje "El Pozo" (3000) Santa Fe, Argentina. E-mail: jvega@santafe-conicet.gov.ar

C. I. Sanseverinatti, M. M. Perdomo, L. A. Clementi, J. R. Vega

Center for Research and Development in Electrical Engineering and Energetic Systems (CIESE, National Technological University, Santa Fe Regional Faculty), Lavaisse 610 (3000) Santa Fe, Argentina.

L. A. Clementi

Institute for Research and Development in Bioengineering and Bioinformatics (IBB, UNER-CONICET), Ruta Provincial 11, Km 10.5, (3100) Oro Verde, Argentina.

Keywords: styrene-butadiene rubber, mass conversion, variable estimation, bias updating, control chart, statistical stability

Abstract

Soft sensors (SS) are of importance in monitoring polymerization processes because numerous production and quality variables cannot be measured online. Adaptive SSs are of interest to maintain accurate estimations under disturbances and changes in operating points. This article proposes an adaptive SS to online estimate the mass conversion in the emulsion copolymerization required for the production of Styrene-Butadiene rubber (SBR). The SS includes a bias term calculated from sporadic laboratory measurements. Typically, the bias is updated every time a new laboratory report becomes available, but this strategy leads to unnecessarily frequent bias updates. The SS includes a statistic-based tool to avoid unnecessary bias updates and reduce the variability of the bias with respect to classical approaches. A control chart (CC) for individual determinations combined with an algorithmic Cusum is used to monitor the statistical stability of the average prediction error. The adaptive SS enables a bias update only when a loss of said statistical stability is detected. Several bias update methods are tested on a simulated industrial train of reactors for the latex production in the SBR process. The best results are obtained by combining the proposed CC-based approach with a previously developed Bayesian bias update strategy.

1. Introduction

Styrene-Butadiene rubber (SBR) is a commodity used primarily in the tire industry. SBR exhibits similar tensile strength, higher ozone resistance and better weatherability than the natural rubber.[1] The first stage in a typical SBR process is the synthesis of a latex through an emulsion copolymerization of styrene (S) and butadiene (B) carried out in a train of continuously-stirred tank reactors (CSTR). All the ingredients are continuously fed into the first reactor of the train (mainly, monomers: S and B; initiator: I; emulsifier: E, chain transfer agent: X; and water: W). Then, the emulsion flows through the other reactors as the copolymerization progresses, and the final latex is obtained in the last reactor.[2] One important variable to be monitored along the copolymerization is the mass fraction of the reacted monomers (or mass conversion) in the last reactor of the train. Mass conversion is a key variable. In fact, a low conversion turns the process inefficient because of low copolymer production and high costs for recovering the non-reacted monomers. On the other hand, too high conversions lead to high branching degrees that can deteriorate the final rubber properties. Unfortunately, industrial online sensors available for mass conversion are affected by drift and fouling, causing frequent service outages. Industry practice is to periodically collect latex samples (e.g., a sample per hour) which are then measured in an analytical laboratory. These offline measurements are quite accurate, but the high measurement delays prevent the implementation of

effective closed-loop strategies. In contrast, some emulsion polymerization variables can be observed from measurements of typical process variables (such as, temperatures, pressures, feed flows, etc.), allowing the monitoring of variables through online sensors. For example, an online sensor based on an artificial neural network (ANN) model was developed for estimating and controlling quality variables in the semibatch Nitrile rubber process.[3] Also, an online sensor based on ANN proved useful for the online estimation of production and quality variables in the continuous SBR process.[4]

A soft sensor (SS) is basically a mathematical model that allows estimating the value of an unmeasured variable from one or more known or online measured process variables. In this sense, an SS is low cost, offers a quick estimation of a non-measurable variable and can also be used to detect failure states in a process.[5] The base mathematical model of an SS can be derived from either first principles or data captured in the process (data-driven SS). Also, SS can be implemented by combining both approaches. Currently, data-driven SS have gained great relevance due to significant advances in data acquisition systems and machine-learning techniques.[5-12]

Unfortunately, SS estimates are always affected by unavoidable errors caused by inaccurate mathematical models, uncertain model parameters, sensor drifts, measurement noises, etc. To compensate for estimation errors, several adaptive techniques have been developed to automatically update an SS. For instance, Urhan and Alakent proposed the use of a multi-model SS together with two learning methods (adaptive moving window and just-in-time learning) that allow the calculation of the weighting factors to be applied to each sub-model.[6] Yuan et al.[8] used a locally-weighted partial least squares (LWPLS) algorithm to design an adaptive SS capable of performing adequately under abrupt or smooth changes in the monitored variable. More recently, Yamada and Kaneko employed Gaussian mixture models to partition large data sets from the process and then build several SS models.[9] The final SS prediction of the monitored variable is obtained by weighting the individual predictions of each model. All these adaptive strategies are aimed at continuously updating the SS to reach more accurate estimates. Many other adaptive SS have been proposed in the literature.[7, 10-12]

Several mathematical models related to the SBR process have been published. Broadhead and Hamielec developed a nonlinear dynamic model for the production of SBR in a CSTR.[13] Almost simultaneously, Gugliotta et al.[2] published the nonlinear dynamic model for a train of CSTRs. This last model included three main modules: a mass balance module (MBM), a molar mass module (MMM), and an energy balance module (EBM). The MBM consists of a set of nonlinear ordinary differential equations that allows the dynamic prediction of several emulsion polymerization

variables, such as the polymerization rates, the reactant concentrations, the phase volumes, the conversion, the mass fraction of styrene bound to the copolymer, etc. The MMM is implemented with another set of nonlinear ordinary differential equations that uses the outputs of the MBM to calculate the number- and weight-average molar masses and the tri- and tetrafunctional branching degrees of the copolymer. In contrast, the EBM is a set of nonlinear algebraic equations that allows the calculation of the refrigerant flow rate required to keep constant the reaction temperature in each reactor of the train. The model was adjusted to reproduce experimental data collected from an industrial plant currently operated by Pampa Energy S.A. in Argentina. More recently, Saldivar-Guerra et al.[14] presented a mechanistic dynamic model for the production of elastomers in trains of CSTRs, where SBR was specifically considered.

Based on the model by Gugliotta et al.[2], adaptive SS-based methodologies have been proposed for monitoring and controlling the production of SBR in a train of CSTRs and for monitoring the quality variables of the product.[15-18] For example, Minari et al.[15] successfully estimated the optimal feed of reagents at intermediate reactors of the train to increase the production of the process without significantly affecting the properties of the latex. The ANN-based SS included two independent ANN blocks for estimating:[4] 1) solid content, polymer production, average particle diameter, and average copolymer composition; and 2) average molecular weight and average branching degrees. The inputs of the SS are the reagent feeds to the first CSTR and the reaction heat in each reactor. Godoy et al.[16] developed an SS for monitoring production and quality variables of the SBR process based on the molar feed flows of 8 reagents fed into the first reactor of the train plus the reaction heat in every reactor. The SS of Minari et al.[4] and Godoy et al.[16] exhibited acceptable performance when tested through simulated examples. Then, Godoy et al.[17] proposed a self-validation strategy for detecting sensor failures in the SBR process.

The last mentioned SSs were not adaptive, thus limiting their applicability in the industry. Sangoi et al.[18] proposed a data-driven adaptive SS based on a linear regression of the molar feed flows of styrene, butadiene, initiator, and the total mass flow of evaporated refrigerant to monitor the mass conversion of the process online. In their work, a novel statistical Bayesian methodology was proposed for adaptation of the SS every time a new laboratory report is available. Nevertheless, the proposed methodology showed deteriorated performance in some particular scenarios, for example, when the process was in a stationary state, the methodology produced unnecessary adaptation in response to random noise of instrumental sensors or due to typical uncertainties in laboratory reports.

In general, industrial processes often use off-line laboratory measurements of samples taken at specific places and times to update SSs according to a pre-specified methodology. However, this classical approach has several drawbacks, such as: low sampling frequencies, uncertainties in sampling times, delays in the availability of the laboratory reports, errors in the laboratory measurements, etc.[5, 19] The prediction error is a key variable for the design, evaluation and maintenance of an SS. For a given process variable (y_t) sampled at time t, the laboratory will provide the measurement result τ minutes later, at time T = $t + \tau$. Then, the prediction error evaluated at the time T, $\varepsilon_{\mathrm{T}}^{\mathrm{p}}$, is defined as:

$$\varepsilon_{\mathrm{T}}^{\mathrm{p}} = \hat{y}_{\mathrm{T}}^{\mathrm{lab}} - \hat{y}_{\mathrm{T}-\tau} \quad (1)$$

where the symbol "^" indicates estimated value of a given variable, $\hat{y}_{\mathrm{T}}^{\mathrm{lab}}$ is the laboratory report available at the time T, and $\hat{y}_{\mathrm{T}-\tau}$ is the estimate of y_t provided by the SS at T- τ. The prediction error can be used to evaluate the inevitable deterioration of the SS performance over time. Said deterioration can be gradual (generally due to some drifts in the sensors or in the process), or abrupt (for example, due to a change in the operating point of the process, the presence of a large disturbance, or a failure of some sensor).[20, 21]

In the process industry, a widely-used procedure for updating an SS is to add a term -the *bias*- to the base mathematical model.[19, 22] Then, the SS estimate is corrected by some bias updating strategy, while the base mathematical model and its parameters remain unchanged over time. In principle, an effective bias updating strategy requires determining not only the magnitude of the update, but also its timing. Most methods update the bias by a magnitude proportional to the current prediction error or its cumulative sum in a given time window (see Appendix).[19] Despite their simplicity, these methodologies have the drawback of requiring the selection of at least one parameter to calculate the magnitude of the update. In addition, the optimal value of the parameter may depend on the operating point of the process, the existence of disturbances in the sensors or in any other parts of the process, the sampling frequency and the level of uncertainty in the laboratory determinations, among others.[18] To mitigate some of these drawbacks, it was proposed to calibrate specific SS models for some typical operating points of the process. Then, the best adaptation strategy was obtained by weighting the incidence of the different models in relation to the actual operating point of the plant.[23, 24] Concerning the timing, it is common to update the bias when a new laboratory report is available.[18, 19, 25, 26] This strategy leads to implement unnecessary bias

updates (e.g., when the process is in a steady state and the prediction error changes due to usual sensor noises or laboratory errors). Furthermore, frequent bias updates can degrade the performance of closed-loop control strategies that use the output of the SS as a feedback signal. Then, it is of interest to develop a statistic-based tool to decide whether or not to implement a bias update each time a new laboratory report becomes available. Therefore, some authors have proposed to update the bias only if: (i) the laboratory measurement is reliable, and (ii) the prediction error exceeds a minimum threshold.[19, 24, 27] In general, confidence in laboratory measurements can be ensured by repeatability and reproducibility studies, equipment calibrations, etc. It has been suggested to set the minimum threshold as $1.96\times\sigma^{cal}$, being σ^{cal} the standard deviation of the prediction error calculated at the calibration stage of the SS.[19] A low bias update rate demonstrates the ability of an adaptive SS to adequately follow changes in process operating conditions. Usually, operators show greater confidence in those SS that have a low bias update rate.[27]

Another problem inherent in bias update strategies is the random nature of the information fed into the SS. At least, three sources of randomness are recognized: (i) the online measurements of the sensors are corrupted by noise, (ii) the laboratory determinations are affected by unavoidable uncertainties, and (iii) the sampling times corresponding to the laboratory reports are inaccurate (time stamping errors). These uncertainties could deteriorate the performance of the SS as a consequence not only of erroneous estimates of the magnitude of the bias updates but also of the time in which they are applied.

Control charts (CC) are typically applied to statistically monitor several process variables. In engineering applications, CC have also been used to detect online sensor faults and to support post-fault detection decisions.[28] Recently, a CC has been used to monitor the error in a process variable by comparing a sensor reading with the prediction of the same variable through a neural network.[29] Similarly, Kazemi et al.[30] analyzed the performance of a set of data-driven SS in the presence of several disturbances and suggested the joint use of standard CC and CC of cumulative sums (Cusum) to detect online failures. The statistical concepts underlying CC are of interest for the development of new process monitoring strategies. For example, a variant of the Cusum method was useful to detect changes in process parameters, even in the presence of non-Gaussian data.[31] As far as the authors are aware, CC have not yet been investigated for strategies aimed at updating the bias of an adaptive SS.

This article proposes an adaptive SS-based methodology specifically designed to monitoring mass conversion in the production of SBR, which avoids the unnecessary bias updates that would be obtained with a classic SS. In the new proposal, a bias update is implemented only when a

statistically significant change in the mean of $\varepsilon_{\mathrm{T}}^{\mathrm{p}}$ is detected. That change is determined from a combination of two complementary CCs. The CCs scheme is coupled with a methodology for bias update also based on $\varepsilon_{\mathrm{T}}^{\mathrm{p}}$. The proposed methodology is evaluated through simulated examples generated on the basis of the first principle model by Gugliotta et al.[2] For comparison, classic SSs that are often used in industrial applications to update the bias are also implemented. All the alternative SSs are evaluated through ad-hoc performance indexes.

2. The Proposed Adaptive Soft Sensor

Figure 1 schematically represents the general structure of the proposed adaptive SS, which includes a basic SS with a bias update term, β_t. The fundamentals of the basic SS and some alternatives to calculate β_t are briefly described in the Appendix. Note that β_t is a piecewise constant function that will be updated at some T only. In fact, the basic idea of the current proposal is to enable the bias update only when a loss of statistical stability in the mean of $\varepsilon_{\mathrm{T}}^{\mathrm{p}}$ is detected at some T. Otherwise, the bias will remain unchanged ($\beta_{\mathrm{T}} = \beta_{\mathrm{T}_{-1}}$).

To monitor the mean of $\varepsilon_{\mathrm{T}}^{\mathrm{p}}$, it is proposed the simultaneous use of two widely used CC: a moving-range CC for individual measurements and a Cusum CC. These two tools are selected for the complementarity of their statistical powers when monitoring the average value of some parameter. In fact, a moving-range CC is efficient at quickly detecting a relatively large change; while Cusum can provide a somewhat delayed alarm but is capable of detecting small gradual changes.

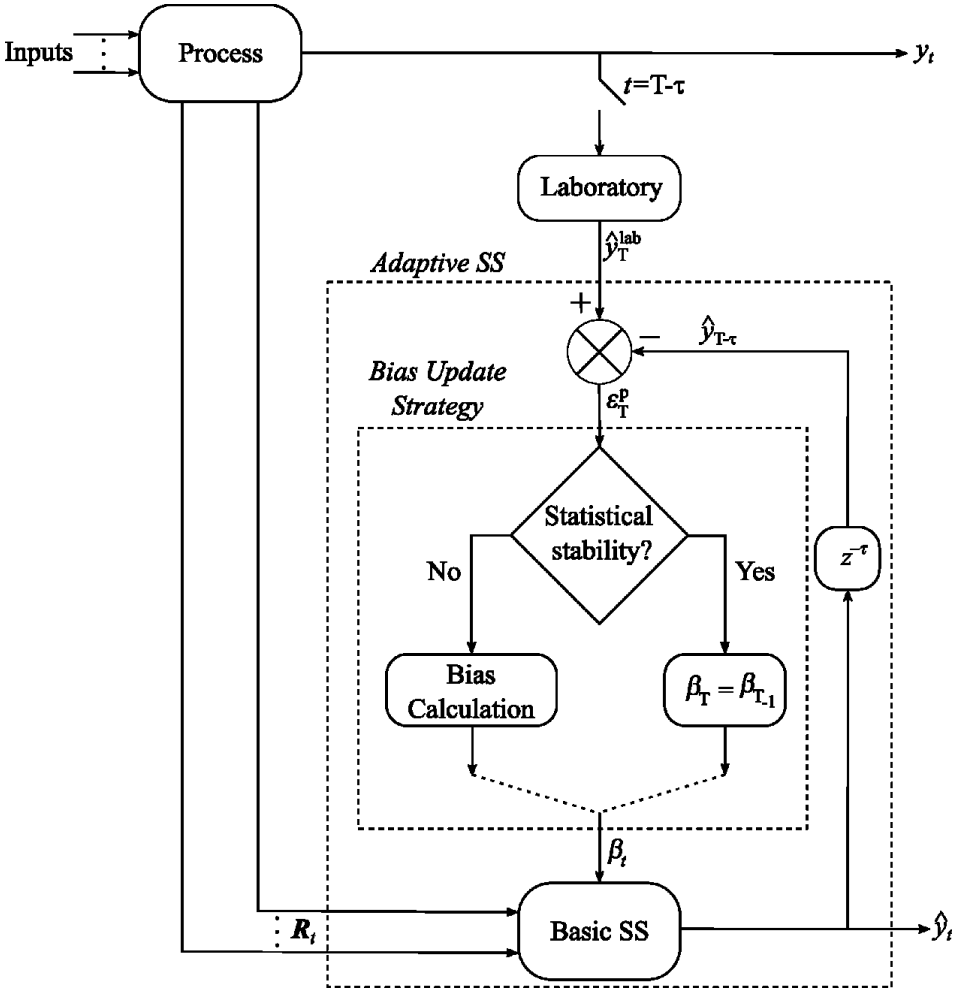

Figure 1. Schematic representation of the proposed adaptive SS for a continuous process.

The efficiency of a CC as a statistical tool is subject to the normality of its input data. In the present case, the normality of $\varepsilon_{\mathrm{T}}^{\mathrm{p}}$ can be ensured in the absence of significant disturbances or sensor failures, and for a fixed operating point. Under such ideal process operation, the following is expected: (i) any of the process measurements, $\mathbf{R}_t$, are affected by unavoidable sensor noises, which in turn could be accepted to follow a Gaussian distribution; and (ii) the laboratory measurements $\hat{y}_{\mathrm{T}}^{\mathrm{lab}}$ follow a Gaussian distribution. Under such conditions, the CC are calibrated to accept the statistical stability of $\varepsilon_{\mathrm{T}}^{\mathrm{p}}$, and therefore no bias update will be necessary (i.e., $\beta_{\mathrm{T}} = 0$). Then, it is expected that $\varepsilon_{\mathrm{T}}^{\mathrm{p}}$, obtained from Equation 1, follows a stable Gaussian distribution along the time. When such statistical stability is lost, then a bias update will be implemented, and Equation A.1 will provide a corrected estimate.

The following two sub-sections describe the implementation of each CC.

2.1. Control Chart for individual measurements

Assuming that $\varepsilon_{\mathrm{T}}^{\mathrm{p}}$ follows a normal statistical distribution, the corresponding control limits and central line are calculated during the calibration stage of the CC under a 3-σ concept, as follows:[32]

$$\text{Upper Control Limit} = \text{UCL} = \bar{\varepsilon}^{\mathrm{p}} + 3\frac{\overline{MR}}{d_2} \quad (2.a)$$

$$\text{Central Line} = \text{CL} = \bar{\varepsilon}^{\mathrm{p}} \quad (2.b)$$

$$\text{Lower Control Limit} = \text{LCL} = \bar{\varepsilon}^{\mathrm{p}} - 3\frac{\overline{MR}}{d_2} \quad (2.c)$$

where $\bar{\varepsilon}^{\mathrm{p}}$ is the average prediction error, $\overline{MR}$ is the second order-average moving range, and d_2 is a factor that allows the estimation of the standard deviation as $\overline{MR}\ /d_2$, as an alternative to the usual definition given by: $\left[\sum_{i=1}^{n}(\varepsilon_i^{\mathrm{p}} - \bar{\varepsilon}^{\mathrm{p}})^2\ /(n-1)\right]^{1/2}$. In fact, for sample sizes smaller than 10 (n < 10), the proposed calculation yields more accurate estimates.[33] The parameters $\bar{\varepsilon}^{\mathrm{p}}$ and $\overline{MR}$ are calculated as follows:

$$\bar{\varepsilon}^{\mathrm{p}} = \frac{1}{\mathrm{E}}\sum_{i=1}^{\mathrm{E}}\varepsilon_i^{\mathrm{p}} \quad (3.a)$$

$$\overline{MR} = \frac{1}{\mathrm{E}-1}\sum_{i=1}^{\mathrm{E}-1}MR_i = \frac{1}{\mathrm{E}-1}\sum_{i=1}^{\mathrm{E}-1}\left|\varepsilon_{i+1}^{\mathrm{p}} - \varepsilon_i^{\mathrm{p}}\right| \quad (3.b)$$

where $\varepsilon_i^{\mathrm{p}}$ (i = 1, …, E) represents the i-th prediction error calculated on the basis of a calibration data set of E samples.

Under the hypothesis of normality of the $\varepsilon_{\mathrm{T}}^{\mathrm{p}}$, the statistical stability of its average value, $\bar{\varepsilon}_{\mathrm{T}}^{\mathrm{p}}$, was determined on the basis of the following four decision rules:[32] 1) one point outside of the control limits; 2) two consecutive points, or two of three consecutive points outside the two-sigma warning limits but still inside the control limits; 3) four consecutive points, or four of five consecutive

points beyond the one-sigma limits; and 4) a run of eight consecutive points on one side of the center line.

2.2. Algorithmic Cusum Control Chart

The one-sided upper and lower Cusum statistics, C_i^+ and C_i^-, respectively, are calculated as follows:[32]

$$C_i^+ = \max\left[0\ ,\ \left(\varepsilon_i^{\mathrm{p}} - \mu_0\right) + C_{i-1}^+\right], \quad \text{(with } C_0^+ = 0\text{)} \tag{4.a}$$

$$C_i^- = \max\left[0\ ,\ \left(\mu_0 - \varepsilon_i^{\mathrm{p}}\right) + C_{i-1}^-\right], \quad \text{(with } C_0^- = 0\text{)} \tag{4.b}$$

where μ_0 is the target value. The statistics C_i^+ and C_i^- accumulate the deviations of the prediction error above and below the target value μ_0, respectively. Thus, in order to detect a small shift in $\varepsilon_{\mathrm{T}}^{\mathrm{p}}$, the target μ_0 is here chosen as the average prediction error obtained from the calibration data set, i.e., $\mu_0 = \bar{\varepsilon}^{\mathrm{p}}$ (Equation 3.a). In principle, the prediction error should be as low as possible, then it is expected $\bar{\varepsilon}^{\mathrm{p}} \cong 0$. The control limit, *H*, is adopted as four times the standard deviation of the prediction error obtained from the calibration data set, i.e., $H = 4\frac{\overline{MR}}{d_2}$ (Equation 3.b). Then, $\varepsilon_{\mathrm{T}}^{\mathrm{p}}$ is assumed to be out of statistical control when either C_i^+ or C_i^- falls outside the control limit; i.e., when $C_i^+ > H$ or $C_i^- > H$. Finally, when an out-of-control is detected, $C_i^+$and C_i^- are reset to $C_i^+/2$ and $C_i^-/2$, respectively.

3. Case of Study

A linear adaptive SS (that includes a bias updating term) will be used to online obtain the estimated mass conversion, $y_t = x_t$, in a SBR process emulated through the model reported by Gugliotta et al.[2] **Figure 2** shows a simplified scheme of the SBR polymerization process carried out in a train of 10 CSTRs. Each reactor has a local refrigerant accumulator that allows the emulsion temperature to be regulated at 10 ºC. The evaporated refrigerant leaving the *i*-th accumulator, $G_{R,i}$, is injected into a collector pipe.

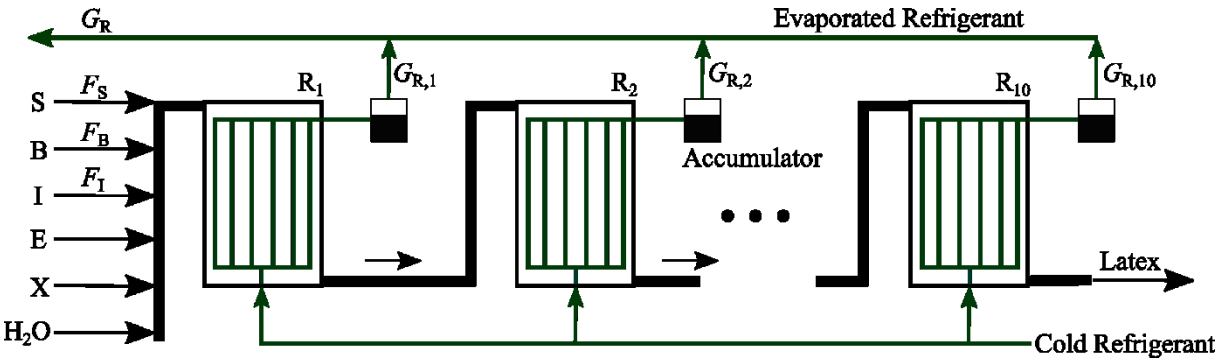

Figure 2. Simplified scheme of the polymerization process. The gray lines indicate the cooling circuit.

The train of reactors operates in a quasi-steady state due to undesirable disturbances or planned changes in demanded polymer production. Each reactor has a volume of 18.000 dm^3. The total mass flow can range from about 200 $dm^3\ min^{-1}$ to 550 $dm^3\ min^{-1}$, depending on the level of production required. An approximate composition of the mass flows of the input reagents is: 10% styrene, 35% butadiene, 30% to 45% water, and 10% to 25% other reagents.

The following (column) vector of measurements is defined (superscript " ′ " indicates vector transpose): $\mathbf{R}_t = [F_{\mathrm{S}_t}\ F_{\mathrm{B}_t}\ F_{\mathrm{I}_t}\ G_{\mathrm{R}_t}]'$, where F_{S_t}, F_{B_t}, and F_{I_t} are the molar flows (of S, B, and I, respectively) fed into the first reactor of the train at time t; and G_{R_t} is the total mass flow of refrigerant consumed by the N_R = 10 reactors of the train, i.e.: $G_{\mathrm{R}_t} = G_{\mathrm{R},1_t} + \cdots + G_{\mathrm{R},\mathrm{N}_{\mathrm{R}_t}}$, where $G_{\mathrm{R},\mathrm{i}_t}$ (i = 1, …, N_R) is the mass flow of refrigerant consumed by the i-th reactor. Even though other available measurements could have been included in $\mathbf{R}_t$ (e.g., the molar flows of E, X, and H_2O), it was preferred to select a minimum amount of variables to achieve a simpler SS. More specifically, the molar flow of X was not included because it has practically no effect on x_t. On the other hand, the E and H_2O feed rates are almost proportional to the I feed rate when the total flow rate is changed to modify the polymer production. If that proportionality is lost, then the adaptive SS will have to compensate for the modeling error. The four chosen variables were also confirmed through a correlation study that pointed to these variables as the most correlated with conversion in this process.

3.1. Mathematical Model of the Soft Sensor

According to the structure of Equation A.1, the linear mathematical model of the proposed inferential sensor is represented through the following multivariate regression:

$$\hat{x}_t = \left(\theta_0 + \theta_1 \tilde{F}_{\mathrm{S}_t} + \theta_2 \tilde{F}_{\mathrm{B}_t} + \theta_3 \tilde{F}_{\mathrm{I}_t} + \theta_4 \tilde{G}_{\mathrm{R}_t}\right) + \beta_t = \left([1 \ \tilde{\mathbf{R}}_t{}'] \cdot \boldsymbol{\Theta}\right) + \beta_t \quad (5)$$

where $\boldsymbol{\Theta} = [\theta_0 \ \theta_1 \ \theta_2 \ \theta_3 \ \theta_4]'$ (5×1) is a vector of unknown parameters, and the symbol "~" refers to a variable contaminated by experimental noise.

The calibration of the SS consists of adjusting the five parameters $\theta_0, \ldots, \theta_4$. To this effect, the detailed mathematical model was used to emulate the synthesis of the commercial degree SBR-1712.[2] For simplicity, it was assumed that the samples to be analyzed in the laboratory were collected at constant intervals of $\Delta \mathrm{T} = 4$ h. Three global latex production levels were adopted from typical industrial recipes in the reactor train (see **Table 1**): 522.2 dm^3 min^{-1}, 386.3 dm^3 min^{-1}, and 227.2 dm^3 min^{-1}, and implemented along the time periods P1 to P3, respectively. First, a period of 1,200 min was used to stabilize the process. For each production level, each feed flow ($F_{\mathrm{S}_t}, F_{\mathrm{B}_t}, F_{\mathrm{I}_t}$) was varied sequentially through pulses of [-10%, 0%, +10%, 0%] with respect to their nominal values. Each pulse lasted 800 minutes. After each change in the production level, an additional stabilization period of 120 minutes was considered. Then, the total simulation time for the three periods was 504 hours, and measurements of samples taken every 4 hours were simulated. Therefore, 127 sets of simulated measurements were obtained. To achieve some polymer quality restrictions, the emulsion temperature in each reactor was set at 10 ºC. Purities of styrene, butadiene and initiator were 98%, 98% and 50%, respectively. All recipes were adjusted to achieve the final specifications of the industrial SBR-1712 in the last reactor: mass conversion ≅ 58%, fraction of styrene bounded to the copolymer ≅ 23%, number-average molar mass ≅ 210,000 g mol^{-1}; weight-average molar mass ≅ 760,000 g mol^{-1}; number-average of trifunctional branching points ≅ 0.19; and number-average of tetrafunctional branching points ≅ 0.08.[2]

Table 1. Reference feed flows (dm^3 min^{-1}) utilized for calibrating the inferential sensor (periods P1, P2, P3, in hours), and for testing the bias updating method (period P4, in hours).

Period	F_{S}	F_{B}	F_{I}	F_{W}	Others[a)]	Total Flow rate
P1: 0 – 168	52.6	185.0	0.12	162.5	122.0	522.2
P2: 169 – 336	39.0	136.8	0.06	139.4	71.0	386.3

P3: 337 – 504	22.7	80.0	0.02	100.5	24.0	227.2
P4: 505 – 654	54.2	190.7	0.40	165.7	126.5	537.5

[a)]Approximate feed flows ($dm^3\ min^{-1}$) of other reagents.

At times T = [T_1, T_2, …] = [4 h, 8 h, …], the simulated values of x_{T} and $\mathbf{R}_{\mathrm{T}}$ were stored. At each sampling time T, the laboratory determination of *x*, $\tilde{x}_{\mathrm{T}}^{\mathrm{lab}}$, was simulated as follows:

$$\tilde{x}_{\mathrm{T}}^{\mathrm{lab}} = x_{\mathrm{T}} + \varepsilon_{\mathrm{T}}^{\mathrm{lab}}(\mu_{\mathrm{lab}}, \sigma_{\mathrm{lab}}) \tag{6}$$

where the simulated laboratory error $\varepsilon_{\mathrm{T}}^{\mathrm{lab}}$ was assumed as a normally distributed random value with mean μ_{lab} = 0 and standard deviation σ_{lab} = 1% of the mean of x_{T}.

The noisy measured variables $\widetilde{\mathbf{R}}_{\mathrm{T}}$ were simulated as follows:

$$\widetilde{\mathbf{R}}_{\mathrm{T}} = \mathbf{R}_{\mathrm{T}} + \boldsymbol{\varepsilon}_{\mathbf{R}}(\boldsymbol{\mu}_{\mathbf{R}}, \boldsymbol{\sigma}_{\mathbf{R}}) \tag{7}$$

where $\boldsymbol{\varepsilon}_{\mathbf{R}}(\boldsymbol{\mu}_{\mathbf{R}}, \boldsymbol{\sigma}_{\mathbf{R}}) = \left[\varepsilon_{F_{\mathrm{S}}}(\mu_{\mathrm{S}}, \sigma_{\mathrm{S}})\ \ \varepsilon_{F_{\mathrm{B}}}(\mu_{\mathrm{B}}, \sigma_{\mathrm{B}})\ \ \varepsilon_{F_{\mathrm{I}}}(\mu_{\mathrm{I}}, \sigma_{\mathrm{I}})\ \ \varepsilon_{G_{\mathrm{R}}}\left(\mu_{G_{\mathrm{R}}}, \sigma_{G_{\mathrm{R}}}\right)\right]'$ is the (column) vector of sensor errors. The error of each sensor was randomly drawn from a zero-mean Gaussian distribution. In the industrial plant, the standard deviation of the refrigerant flow meter signal is approximately three times the standard deviations of the other flow meters. Then, the simulated standard deviations were 1% (for $F_{\mathrm{S}_t}, F_{\mathrm{B}_t}, F_{\mathrm{I}_t}$) and 3% (for G_{R_t}), with respect to the means of their respective signals.

Finally, the 127 simulated pairs $\left(\tilde{x}_{\mathrm{T}}^{\mathrm{lab}}, \widetilde{\mathbf{R}}_{\mathrm{T}}\right)$ were utilized for the calibration of the inferential model of Equation 5. The parameters $\boldsymbol{\Theta}$ (5×1) were estimated through a standard least squares procedure, i.e.:

$$\boldsymbol{\Theta} = (\mathbb{R}'\,\mathbb{R})^{-1}\,\mathbb{R}'\,\mathbf{X} \tag{8}$$

where $\mathbf{X} = [\tilde{x}_{\mathrm{T}_1}^{\mathrm{lab}} \;\; \tilde{x}_{\mathrm{T}_2}^{\mathrm{lab}} \;\; \ldots \;]'$ (127×1) is a vector that contains the noisy laboratory values, and $\mathbb{R}$ (127×5) is a matrix whose *i*-th row is the augmented row vector of noisy inputs, $[1 \; \tilde{F}_{\mathrm{S}_{T_i}} \; \tilde{F}_{\mathrm{B}_{T_i}} \; \tilde{F}_{\mathrm{I}_{T_i}} \; \tilde{G}_{R_{T_i}}]$. From Equation 8, the following parameters were obtained: $\boldsymbol{\Theta} = [0.6058 \;\; 8.573 \;\; -0.0008 \;\; 0.3790 \;\; 0.0002]'$. These parameters resulted in a R^2 value of 0.52, with p-values of approximately 0, 0.014, 0.010, 0.150, and 0.040, respectively, indicating statistical significance for all regression variables. It is important to note that the modeled process is nonlinear, the calibration data includes different production levels and is contaminated with significant noises. Under these considerations, the obtained multivariate linear regression model is acceptable.

3.2. Calibration of the Control Charts

The prediction error was calculated from the calibration data set, as follows:

$$\boldsymbol{\varepsilon}^{\mathrm{p}} = \begin{bmatrix} \varepsilon_{\mathrm{T}_1}^{\mathrm{p}} \\ \vdots \\ \varepsilon_{\mathrm{T}_{127}}^{\mathrm{p}} \end{bmatrix} = \begin{bmatrix} \tilde{x}_{\mathrm{T}_1}^{\mathrm{lab}} \\ \vdots \\ \tilde{x}_{\mathrm{T}_{127}}^{\mathrm{lab}} \end{bmatrix} - \begin{bmatrix} 1 & \tilde{F}_{\mathrm{S}_{\mathrm{T}_1}} & \tilde{F}_{\mathrm{B}_{\mathrm{T}_1}} & \tilde{F}_{\mathrm{I}_{\mathrm{T}_1}} & \tilde{G}_{\mathrm{R}_{\mathrm{T}_1}} \\ & & \vdots & & \\ 1 & \tilde{F}_{\mathrm{S}_{\mathrm{T}_{127}}} & \tilde{F}_{\mathrm{B}_{\mathrm{T}_{127}}} & \tilde{F}_{\mathrm{I}_{\mathrm{T}_{127}}} & \tilde{G}_{\mathrm{R}_{\mathrm{T}_{127}}} \end{bmatrix} \begin{bmatrix} \theta_0 \\ \theta_1 \\ \theta_2 \\ \theta_3 \\ \theta_4 \end{bmatrix} = \mathbf{X} - \mathbb{R}\,\boldsymbol{\Theta} \tag{9}$$

The 127 values of $\boldsymbol{\varepsilon}^{\mathrm{p}}$ are represented by dots in **Figure 3a**. Although the calibration set includes different operating conditions (mainly different production rates), the prediction error exhibits a random behavior in any period. Figure 3b shows a Q-Q plot for the prediction error of Figure 3a. The straight trend shown in Figure 3b suggests an underlying Gaussian distribution for $\varepsilon_{\mathrm{T}}^{\mathrm{p}}$. From Figure 3a, the average value of the prediction error is close to zero and the standard deviation is 0.79.

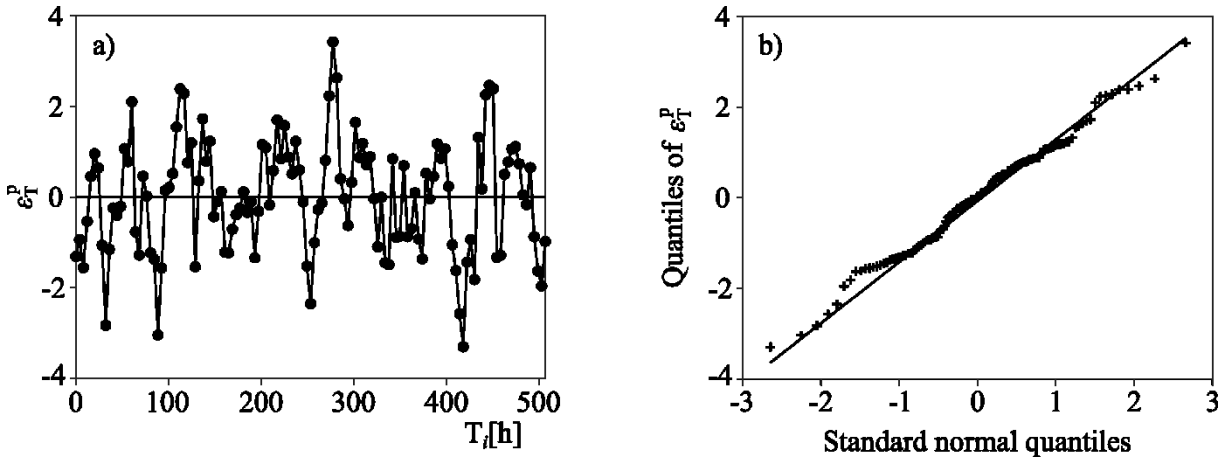

Figure 3. a) Prediction error corresponding to the whole calibration data set. b) Q-Q plot for the prediction error.

To calibrate the CCs, the first step was to detect and exclude outliers and out-of-control points in the data set. Ten points were excluded because they all violated at least one of the four decision rules. Then, the procedures of sections 2.1 and 2.2 were applied to obtain the control limits corresponding to the CC for individual measurements and the parameters μ_0 and H for the Cusum CC. The following values were obtained: CL = 0; LCL = -2.4; UCL = 2.4; $\mu_0 = 0$; and H = 3.16 (strictly, $\mu_0 < 0.02$ was obtained during the calibration stage). Also, the constant d_2 adopts the value 1.128, which corresponds to the two samples used for the calculation of every moving range.[32]

3.3. Simulation of the SBR Train with the Adaptive Soft Sensor

To evaluate the adaptive SS, the recipe of period P4 (see Table 1) was simulated along 150 h. The measured variables were assumed to be acquired at time intervals Δt = 1 min. Every 4 h, a laboratory determination $\tilde{x}_T^{lab}$ was simulated through Equation 6, and the measurement report was affected by a delay time τ = 2 h. The time stamping error was randomly sampled from a zero-mean Gaussian distribution of standard deviation 0.25 h. The mass conversion in the last reactor of the train was estimated through Equation 5; and the bias β_t was updated according to the procedure described in Figure 1.

Table 2 details the reference case (C_1) and five scenarios (C_2 to C_6) that include process disturbances and sensor failures. The reference case C_1 keeps the operating conditions of P4 unchanged, without including process disturbances or sensor errors. Case C_2 simulates simultaneous abrupt reductions of all the reactant feed rates at 5,250 min, with a decrease of the total latex feed rate from 537 $dm^3\ min^{-1}$ to 511 $dm^3\ min^{-1}$. Case C_3 considers a sudden reduction of 5% in the purity

of the initiator, at 4,000 min. Case C_4 simulates a failure in the cooling system of Reactor 5 that causes a temperature increase from 10 °C to 15 °C, at 5,250 min. Case C_5 assumes an increasing linear drift (0.01 % min^{-1}) in the signal transmitted by the sensor of F_{S_t}, from 4,000 min to 6,500 min. Case C_6 assumes an off-set of +15% in the signal transmitted by the sensor of G_{R_t}, from 4,000 min to 6,500 min. Every disturbance C_2 to C_6 was implemented starting from the reference case, C_1. Note that C_2, C_3 and C_4 produce a transition to a different final value of x_t. In contrast, C_5 and C_6 correspond to errors in the transmitted measured signals, while x_t remains unaffected.

Table 2. Simulated scenarios along the period P4.

Case	Disturbance or Sensor Failure	Affected variables
C_1	Reference case (no disturbance)	-
C_2	Latex feed rate: from 537 dm^3 min^{-1} to 511 dm^3 min^{-1}	F_{S_t}, F_{B_t}, F_{I_t}
C_3	Initiator purity: 5% undetected reduction	F_{I_t}
C_4	Temperature of Reactor 5: 5 °C rise	G_{R_t}
C_5	Sensor of F_{S_t}: Undetected linear drift (+0.01 % min^{-1})	F_{S_t}
C_6	Sensor of G_{R_t}: Undetected offset (+15%)	G_{R_t}

The mass conversion x_t was estimated through the method proposed in Figure 1. For comparison, the following bias updating algorithms were implemented: (i) the classical approach of Equation A.2a, with α ranging from 0 to 1 in steps of 0.05; (ii) the cumulative sum approach of Equation A.2b with n = 4 as a typical value (also with α from 0 to 1 in steps of 0.05); and (iii) the Bayesian approach of Equation A.3 with k = 2.[18] Additionally, to study the impact of the proposed CC strategy, the results were compared to those obtained through approaches i), ii) and iii) without considering any CC.

The (positive) true relative error in the estimated conversion is defined as follows:

$$\varepsilon_{T_i}^{t} = \left| \frac{x_{T_i} - \hat{x}_{T_i}}{x_{T_i}} \right| \tag{10}$$

Three indexes were defined to evaluate the performance of all bias updating methods: 1) $\bar{\varepsilon}$: average value of $\varepsilon_{\mathrm{T}_i}^{\mathrm{t}}$; 2) N_{bu}: number of bias updates; and 3) σ_β: standard deviation of the bias updates.

$$\bar{\varepsilon} = \frac{1}{N}\sum_{i=1}^{N} \varepsilon_{\mathrm{T}_i}^{\mathrm{t}} \tag{11.a}$$

N_{bu} = number of times that $\beta_i \neq \beta_{i-1}$, (i = 2, …, N) (11.b)

$$\sigma_\beta = \frac{1}{N\, d_2}\sum_{i=2}^{N} |\beta_i - \beta_{i-1}| \tag{11.c}$$

where N = 32 is the number of simulated laboratory reports along the last 128 hours of the period P4 (the first 22 h of P4 were used to stabilize the numerical solutions). Note that the index $\bar{\varepsilon}$ can be computed only when the true mass conversion is known. Although this is not possible in a practical application, this index was used in the simulated examples to assess the capabilities of the studied methods to estimate the true conversion, x_t.

4. Main Results and Discussion

Main results are summarized in **Figure 4** to **Figure 7** and **Table 3**. The following nomenclature is used to refer to the bias update methodologies: “cl” for the classical method of Equation A.2a; “cs” for the cumulative sum method of Equation A.2b; and “by” for the Bayesian method of Equation A.3. Then, “cl-cc”, “cs-cc”, and “by-cc” are used for the corresponding CC-based methods.

For all cases C_1 to C_6, Figure 4 and **Figure 5** respectively show the indexes $\bar{\varepsilon}$ and N_{bu} for every update method, as a function of the parameter α. The analysis of such figures indicates that there is not a given α that minimizes the indexes; on the contrary, the optimum α depends on both the case and the method. For the Bayesian method, constant values of $\bar{\varepsilon}$ are observed because such method is independent of α.

The simulation results of Figure 4 and Figure 5 show the advantages of incorporating a CC to monitor the prediction error and improve the performance of the adaptive SS. For the α-dependent methods, the inclusion of a CC reduces not only the magnitude of the index $\bar{\varepsilon}$ but also its sensitivity to α (Figure 4). Then, the CC ensure low values of $\bar{\varepsilon}$ in any method, for a relatively wide range of values of α. Particularly, note that the performance of the "by-cc" method (no α required) is similar to the performances of methods "cl-cc" and "cs-cc" with the optimum α (see Figure 4). Figure 5 clearly indicates that N_{bu} diminishes when CC are used (without CC, N_{bu} = 32 because the bias is updated after each laboratory report). Thus, a N_{bu} < 32 indicates that 32-N_{bu} unnecessary bias updates have been avoided.

In an ideal case without perturbations in the process (case C_1), no bias update is expected to be required. This would only happen when the classical methods "cs" and "cl" operate with the optimum parameter α = 0 (Figure 4a and 5a). However, this is an unreal operating condition, since Figure 4 alerts on the impossibility of selecting a common optimum value for α that is effective for all cases. In fact, the minimum $\bar{\varepsilon}$ depends on both the case and the bias update method. Particularly, note that the optimum α can range from 0 (case C_1) to 0.95 (case C_3 with "cs-cc", or C_6 with "cl-cc").

In practice, it is impossible to determine the optimal values of α. For this reason, the remaining results were simulated with α = 0.3, as is often suggested in industrial applications.[19] Table 3 summarizes the performance indexes. Almost all the performance indexes show an advantage when using CC (the only exception detected is $\bar{\varepsilon}$ in C_6, but those values are similar with or without CC). The most conclusive results focus on the N_{bu} and σ_β indexes, whose values are significantly lower when CC are used.

For simplicity, cases C_2 and C_6 were selected to show the remaining results. **Figure 6** shows the resulting biases β_t obtained through all methods. Although the overall trends are quite similar, the biases show less variability when CC are used (Figure 6b and 6d). This is mainly observed in the first 5250 minutes for C_2 and the first 4000 minutes for C_6, when there are no disturbances or changes that affect the process. These results are particularly highlighted by the lower values of σ_β (see Table 3). As a consequence of the similar tendencies of the biases, the estimates $\hat{x}_T$ obtained through the different methods are quite similar. As an example, Figure 7 shows the results corresponding to the "cl" and "by" methods.

Finally, it is worthwhile notice that the utilization of CC-based approach "by-cc" improves the performance with respect to "by", evidenced through a decreased in almost all performance indexes (Table 3). The optimization problems required in the Bayesian methods were solved by an initial

golden section search followed by a parabolic interpolation algorithm.[34] In all the analyzed cases, C_1 to C_6, the required computation times were negligible (< 10 msec, on a standard PC with an i7 processor and 8 GB of RAM). Furthermore, the optimization problem proved to be robust, with no convergence problems in multiple runs.

Table 3. Performance indexes (with α = 0.3 in the cl, cl-cc, cs, and cs-cc methods).

		cl	cl-cc	cs	cs-cc	by	by-cc
	$\bar{\varepsilon}\times10^2$	0.5	0.4	0.6	0.4	0.7	0.4
C_1	N_{bu}	32	2	32	4	32	2
	$\sigma_\beta\times10^3$	1.3	0.1	1.1	0.1	1.6	0.2
	$\bar{\varepsilon}\times10^2$	1.6	1.5	1.9	1.7	1.3	0.9
C_2	N_{bu}	32	12	32	10	32	7
	$\sigma_\beta\times10^3$	3.3	2.3	3.2	2.4	3.8	2.4
	$\bar{\varepsilon}\times10^2$	0.8	0.7	1.0	0.9	0.8	0.7
C_3	N_{bu}	32	10	32	7	32	4
	$\sigma_\beta\times10^3$	1.5	0.6	1.4	0.5	1.9	0.5
	$\bar{\varepsilon}\times10^2$	0.6	0.6	0.7	0.7	0.7	0.6
C_4	N_{bu}	32	4	32	7	32	3
	$\sigma_\beta\times10^3$	1.5	0.4	1.1	0.3	1.8	0.4
	$\bar{\varepsilon}\times10^2$	0.5	0.4	0.7	0.4	0.7	0.4
C_5	N_{bu}	32	4	32	4	32	4
	$\sigma_\beta\times10^3$	1.3	0.0	1.1	0.1	1.6	0.2
	$\bar{\varepsilon}\times10^2$	0.9	0.9	1.0	1.1	0.9	0.9
C_6	N_{bu}	32	8	32	12	32	6
	$\sigma_\beta\times10^3$	1.6	0.6	1.4	0.8	1.9	0.8

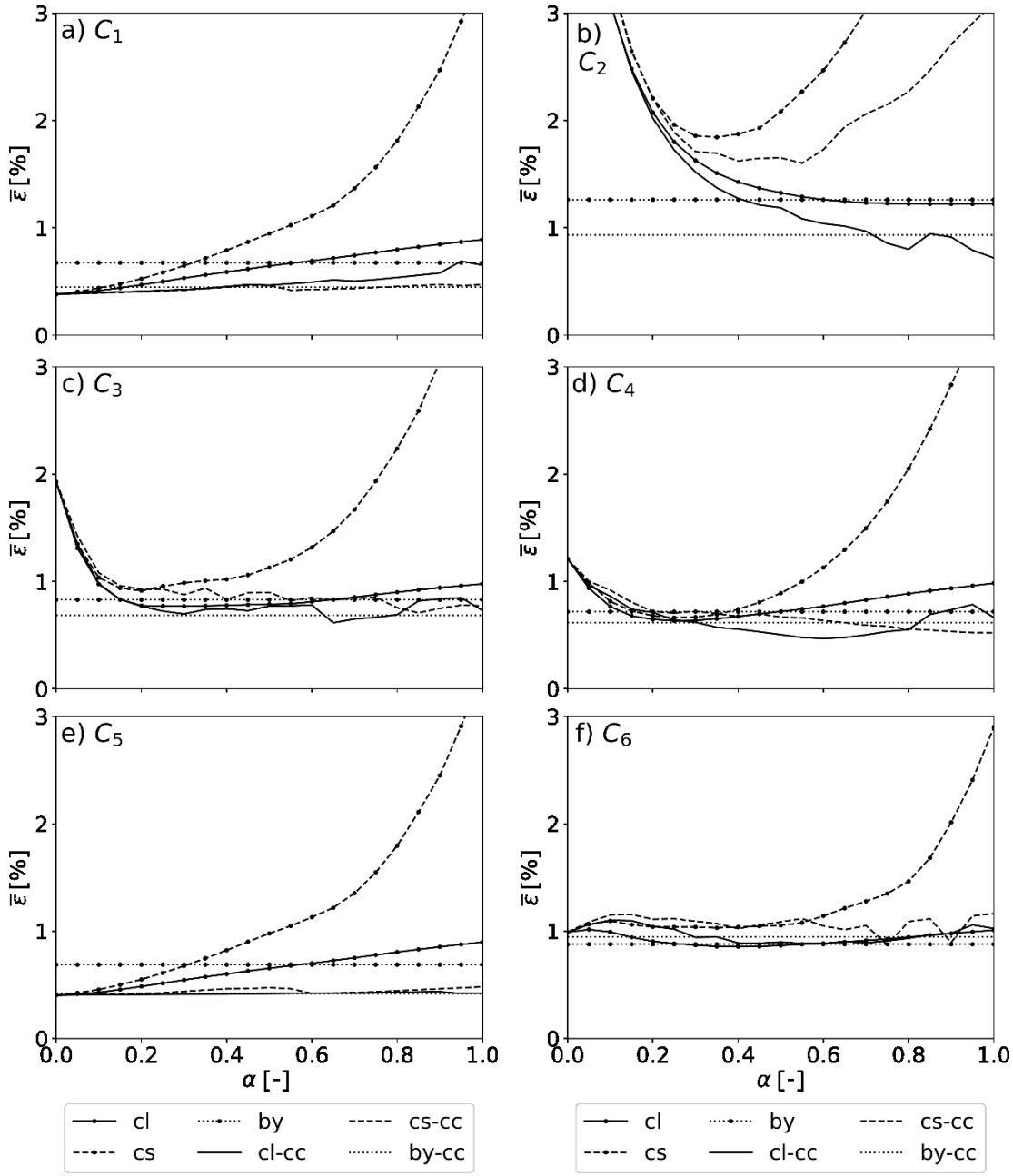

Figure 4. Performance index $\bar{\varepsilon}$ as a function of parameter α, for every case and methodology. Bayesian algorithms are independent of α (horizontal lines for “by” and “by-cc”).

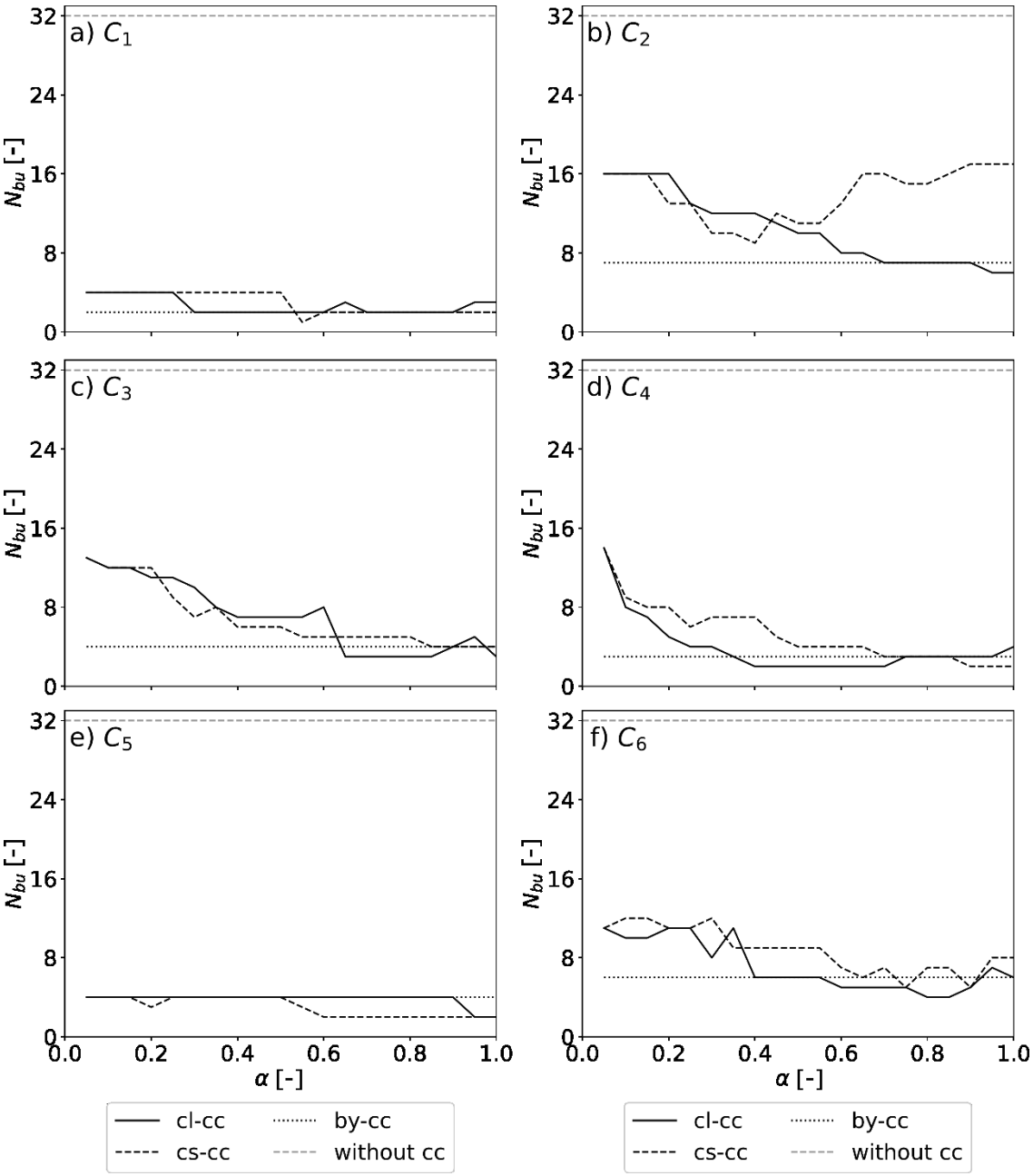

Figure 5. Comparison of N_{bu} as determined through the CC monitoring of the prediction error, as a function of parameter α. For the Bayesian algorithms, N_{bu} is independent of α.

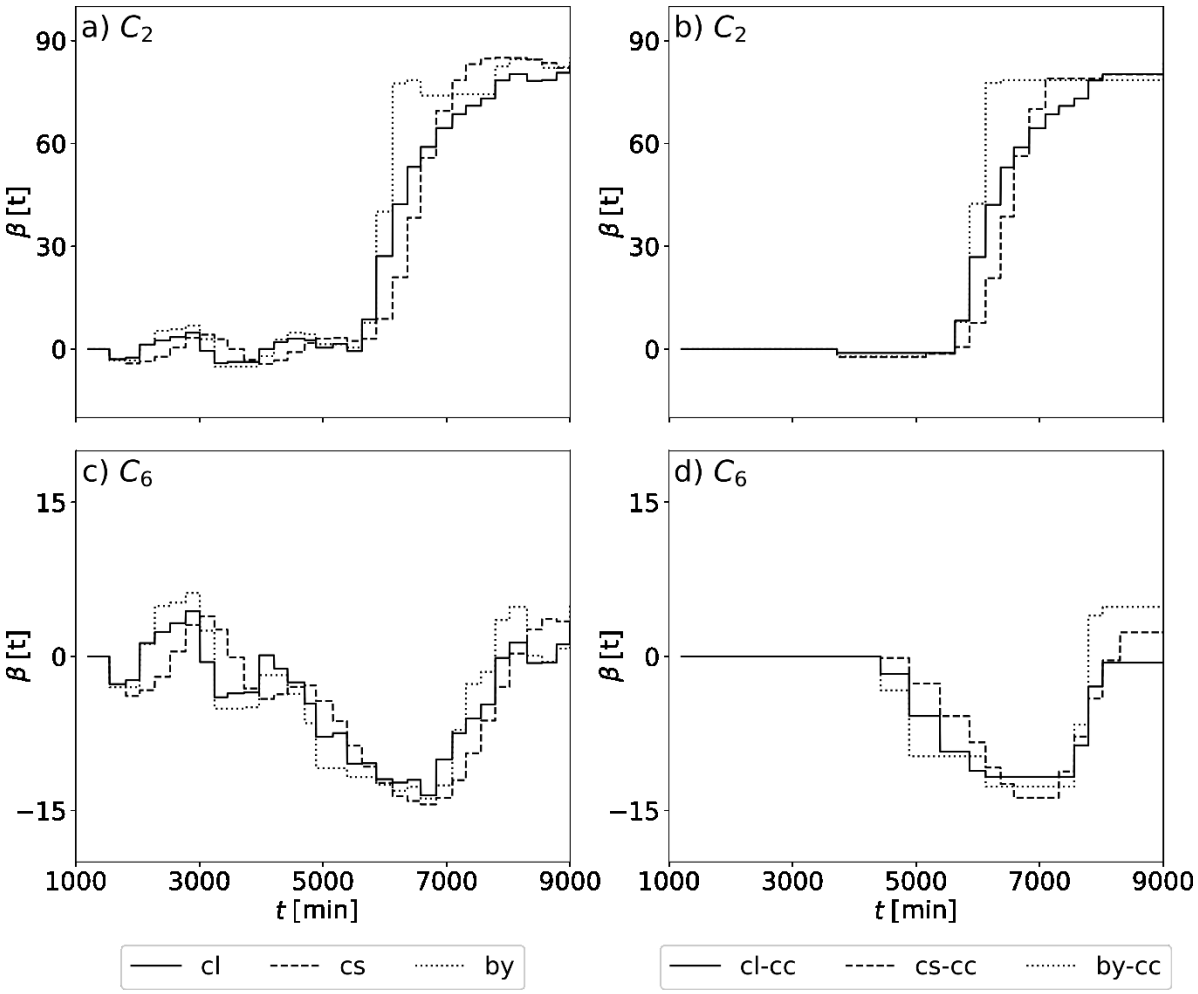

Figure 6. Comparison of biases obtained through the studied methodologies (α = 0.3 was used in the α-dependent methods).

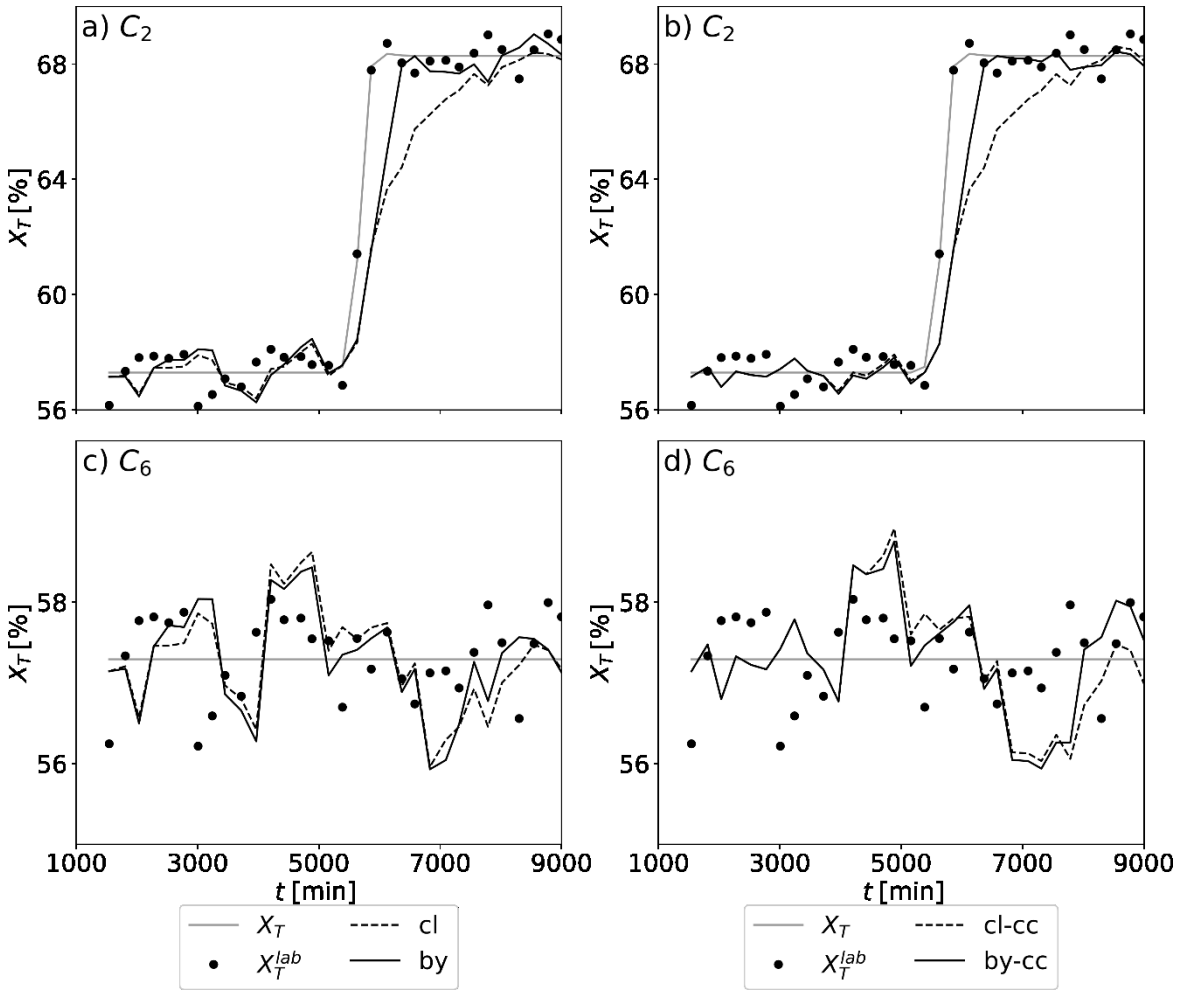

Figure 7. "True" mass conversion x_t, simulated laboratory determinations $\tilde{x}_T^{lab}$, and estimations obtained through the studied methodologies (α = 0.3 was used in the α-dependent methods).

5. Conclusions

The proposed adaptive SS was effective to estimate the mass conversion in all the considered scenarios C_1 to C_6, including free-error steady state conditions, changes in the reactant feed rates (i.e., changes in the plant operating point), presence of unmeasured impurities in the reactants, failures in the cooling system, and failures in the sensors.

The proposed tool utilized online (or high-frequency) measurements of process variables and sporadic (or low-frequency) laboratory measurements of samples of the estimated variable. The SS enabled the bias update only when a loss of statistical stability of the prediction error is detected. The resulting adaptive SS was effective in keeping a low average prediction error, even using fewer bias updates than those resulting from classical methodologies. In addition, less variability in the bias

pattern was achieved. This advantage is of particular interest when a process operates in closed loop using feedback from the SS outputs.

The statistic monitoring through CC revealed a secondary positive effect on any classic SS, given by a decrease in the sensitivity of the SS to the parameter α. Anyway, from a practical point of view, the proposed methodology applied to the Bayesian approach seems to be preferable. In fact, this method does not require the adoption of any parameters. Furthermore, in the current proposal, both the magnitudes and timing of the bias updates result from a fully probabilistic approach that takes into account the random nature of the sensor signals and laboratory reports.

The adaptive SS of Figure 1 can be easily implemented in the industrial plant. The required online measurements are the styrene, butadiene, and initiator flows fed into the first reactor, and the total flow of refrigerant demanded by the train. In addition, the sporadic laboratory measurements are necessary. The first stage consists of calibrating the SS through Equation 8. The second stage is the CC calibration (as described in section 3.2). Then, the adaptive SS of Equation 5 is implemented with the bias β_{Γ} obtained from some of the methods described in the Appendix.

Bias correction through Equation A.1 is able to compensate for deviations in the average value of the prediction error. However, the current strategy is unable to correct for a possible deterioration in the variability of the prediction error. This would require a more general methodology, including some effective CC to monitor variability (e.g., a moving range CC) and an adaptive SS capable of compensating for an increase in the variability of the prediction error (e.g., an SS on-line recalibration). These aspects deserve further investigations.

Appendix. The Basic Soft Sensor and some Methods for Bias Calculation

The mathematical model of an SS with a bias term that is used to monitor a given variable y_t at any time t, can be written as follows:

$$\hat{y}_t = f(\mathbf{R}_t, \mathbf{\Theta}) + \beta_t \qquad \text{(A.1)}$$

where the symbol "^" indicates estimated value of a given variable; $f(\mathbf{R}_t, \mathbf{\Theta})$ is the base mathematical model of the ideal (error-free) SS, which utilizes information taken from J online

measured process variables $\mathbf{R}_t = [r_1(t) \cdots r_{\mathrm{J}}(t)] = [r_{1_t} \cdots r_{\mathrm{J}_t}]$, and includes a set of L parameters $\mathbf{\Theta} = [\theta_1 \ \cdots \ \theta_{\mathrm{L}}]$; and β_t is the bias, typically a piecewise constant function that must be chosen to minimize the unavoidable modeling error (i.e., with the goal of reaching $\hat{y}_t \cong y_t$).[19]

The bias can be calculated on the basis of either the instantaneous prediction error or a cumulative sum of the prediction errors, i.e.:[19]

$$\beta_{\mathrm{T}} = \beta_{\mathrm{T}_{-1}} + \alpha\, \varepsilon_{\mathrm{T}}^{\mathrm{p}}; \quad (0 \le \alpha \le 1) \tag{A.2a}$$

$$\beta_{\mathrm{T}} = \beta_{\mathrm{T}_{-1}} + \alpha \left(\frac{6}{n(n+1)(n+2)} \sum_{i=1}^{n} i(n-i+1)\ \varepsilon_{\mathrm{T}_{-(i-1)}}^{\mathrm{p}} \right); \quad (0 \le \alpha \le 1) \tag{A.2b}$$

where the parameter α and the number of past measurements to be included in the calculation of Equation A.2b, *n*, must be previously chosen. A subscript 'T_{-i}' in a given variable indicates the value of that variable at the *i*-th sampling time previous to T.[18] Thus, for *n* = 1, Equation A.2b becomes Equation A.2a.

Calculation of the bias through Equation A.2a and A.2b has several drawbacks. In fact, the performance of the SS is highly sensitive to the chosen values of α and *n*; furthermore, the optimal values that minimize the modeling errors can be highly dependent on the particular operating conditions of the process.[18] Besides, Equation A.2a and A.2b are deterministic, and therefore overlook the statistical attributes of the prediction error, which are in turn caused by the laboratory determinations $\hat{y}_{\mathrm{T}}^{\mathrm{lab}}$ and the measurements $\mathbf{R}_t$.

A Bayesian inference method has been developed to update the bias each time a new laboratory report becomes available.[18] The magnitude of the bias is calculated by solving the following optimization problem:

$$\max_{\beta_{\mathrm{T}}} \left\{ -\frac{1}{2\,\sigma_{\mathrm{p}}^2\,k} \left[\varepsilon_{\mathrm{T}_{-(\mathrm{k}-1)}}^{\mathrm{p}} + \cdots + \varepsilon_{\mathrm{T}_{-1}}^{\mathrm{p}} + \hat{y}_{\mathrm{T}}^{\mathrm{lab}} - (f(\mathbf{R}_{\mathrm{T}-\tau}, \mathbf{\Theta}) + \beta_{\mathrm{T}}) - k\,\mu_{\mathrm{p}} \right]^2 - \frac{1}{2\sigma_{\beta}^2} \left[\beta_{\mathrm{T}} - \mu_{\beta} \right]^2 \right\} \tag{A.3}$$

where *k* is an adopted constant (typically, *k* = 2 or 3); and μ_{p}, σ_{p}, μ_{β} and σ_{β} are calculated on the basis of historical values of the prediction error, i.e. $\varepsilon^{\mathrm{p}}_{\mathrm{T-K}}, \cdots, \varepsilon^{\mathrm{p}}_{\mathrm{T}_{-1}}$ (K >> *k*). This approach has produced better results than those based on Equation A.2a and A.2b.

Acknowledgements

The authors acknowledge the financial support by CONICET (PIP 251-2015), UTN (PID 5151-2019, PID 8414-2021), IBB (UNER-CONICET), and CIESE (UTN).

Conflict of Interest

The authors declare no conflict of interest.

Received: ((will be filled in by the editorial staff))
Revised: ((will be filled in by the editorial staff))
Published online: ((will be filled in by the editorial staff))

References

[1] G. Odian, *Principles of Polymerization, Fourth Edition*, John Wiley & Sons Ltd, USA **2004**.

[2] L.M. Gugliotta, M.C. Brandolini, J.R. Vega, E.O. Iturralde, J.L. Azum, G.R. Meira, *Polym. React. Eng.* **1995**, *3*, 201.

[3] L.A. Clementi, R.B. Suvire, F.G. Rossomando, J.R. Vega, *Macromol. React. Eng.* **2018**, *12*, 1700054.

[4] R. Minari, G. Stegmayer, L.M. Gugliotta, O.A. Chiotti, J.R. Vega, *Macromol. React. Eng.* **2007**, *1*, 405.

[5] L. Fortuna, S. Graziani, A. Rizzo, M.G. Xibilia, *Soft Sensors for Monitoring and Control of Industrial Processes, first ed.*, Springer-Verlag London, UK **2007**.

[6] A. Urhan, B. Alakent, *Neurocomputing* **2020**, *329*, 23.

[7] J. Ni, S. Li, *Chem. Eng. Sci.* **2021**, *230*, 116210.

[8] X. Yuan, J. Zhou, Y. Wang, *Chemom. and Intell. Lab. Syst.* **2020**, *197*, 103921.

[9] N. Yamada, H. Kaneko, *Chemom. and Intell. Lab. Syst.* **2021**, *219*, 104443.

[10] Z. Liu, Z. Ge, G. Chen, Z. Song, *Contr. Eng. Pract.* **2018**, *72*, 19.

[11] S. V. Vijayan, H.K. Mohanta, A.K. Pani, *Petroleum Sci.* **2021**, *18*, 1230.

[12] M. Siegl, V. Brunner, D. Geier, T. Becker, *Eng. in Life Sci.* **2022**, *22*, 1.

[13] T.O. Broadhead, A.E. Hamielec, *Die Makromol. Chem.* **1985**, *10*, 105.

[14] E. Saldivar-Guerra, R. Infante-Martinez, J.M. Islas-Manzur, *Processes* **2020**, *8*, 1508.

[15] R. Minari, J.R. Vega, L.M. Gugliotta, G.R. Meira, *Ind. Eng. Chem. Res.* **2006**, *45*, 245.

[16] J.L. Godoy, R.J. Minari, J.R. Vega, J.L. Marchetti, *Chem. Int. Lab. Systems.* **2011**, *107(2)*, 258.

[17] J.L. Godoy, J.L. Marchetti, J.R. Vega, *J. Proc. Control* **2017**, *50*, 56.

[18] E. Sangoi, C.I. Sanseverinatti, L.A. Clementi, J.R. Vega, *Comp. Chem. Eng.* **2021**, *147*, 107250.

[19] M. King, *Statistics for Process Control Engineers: A Practical Approach, first. ed.*, John Wiley & Sons Ltd, USA **2017**.

[20] P. Kadlec, B. Gabrys, R. Grbic, *Comput. Chem. Eng*. **2011**, *35*, 1.

[21] Y. Jiang, S. Yin, J. Dong, O. Kaynak, *Control and Optimization of Industrial Processes* **2021**, *21(11)*, 12868.

[22] A.D. Quelhas, J.C. Pinto, *IFAC Proceedings Volumes* **2009**, *42*, 679.

[23] W. Ni, S.D. Brown, R. Man, *Chem. Eng. Sci.* **2014**, *111*, 350.

[24] S. Khatibisepehr, B. Huang, F. Xu, A. Espejo, *J. of Proc. Contr.* **2012**, *22*, 1913.

[25] L. Xie, Y. Zhao, D. Aziz, X. Jin, L. Geng, E. Goberdhansingh, F. Qi, B. Huang, *J. of Proc. Contr.* **2013**, *23*, 990.

[26] Y. Miao, F. Xu, Y. Zheng, B. Huang, J. MacGowan, A. Espejo, *IFAC-PapersOnLine* **2015**, *48*, 63.

[27] M. Mojto, K. Ľubušký, M. Fikar, R. Paulen, *Comp. & Chem. Eng.* **2021**, *135*, 107437.

[28] M. Thomann, L. Rieger, S. Frommhold, H. Siegrist, W. Gujer, *Water Sci. & Tech.* **2002**, *46*, 107.

[29] F. Cecconi, D. Rosso, *Environ. Sci. Technol.* **2021**, *55*, 10064.

[30] P. Kazemi, C. Bengoa, J.P. Steyer, J. Giralt, *Proc. Safety and Environm. Protect.* **2021**, *146*, 905.

[31] N. Saengsura, S. Sukparungsee, Y. Areepong, *Intell. Automat. & Soft Comp.* **2021**, *31*, 635.

[32] D.C. Montgomery, *Introduction to Statistical Quality Control, sixth ed.*, John Wiley & Sons Ltd, USA **2009**.

[33] W.H. Woodall, D.C. Montgomery, *Quality Engineering* **2000**, *13(2)*, 211.

[34] W.H. Press, S.A. Teukolsky, W.T. Vetterling, B.P. Flannery, *Numerical Recipes. The Art of Scientific Computing, third ed.,* Cambridge University Press, USA **2007**.

Summary for the Table of Contents

An adaptive soft sensor (SS) is proposed to estimate the mass conversion in the continuous emulsion copolymerization of styrene and butadiene carried out in an industrial train of reactors. The bias term of the SS is updated when a loss of statistical stability is detected. The best simulation results are obtained when the bias is updated using a Bayesian approach.

Authors:

C. I. Sanseverinatti, M. M. Perdomo, L. A. Clementi, J. R. Vega*

Tittle:

An Adaptive Soft Sensor for On-Line Monitoring the Mass Conversion in the Emulsion Copolymerization of the Continuous SBR Process

Eye-catching figure: